Original Article

JOURNAL OF REINFORCED PLASTICS & COMPOSITES

Journal of Reinforced Plastics and Composites
2015, Vol. 34(16) 1273–1286
© The Author(s) 2015
Reprints and permissions:
sagepub.co.uk/journalsPermissions.nav
DOI: 10.1177/0731684415573980
jrp.sagepub.com

SAGE

Design and fabrication of multi-walled hollow nanofibers by triaxial electrospinning as reinforcing agents in nanocomposites

Jamal Seyyed Monfared Zanjani[1], Burcu Saner Okan[2], Yusuf Ziya Menceloglu[1] and Mehmet Yildiz[1]

Abstract

Multi-walled triaxial hollow fibers with two different outer wall materials are fabricated by core-sheath electrospinning process and integrated into epoxy matrix with or without primary glass fiber reinforcement to produce composites with enhanced mechanical properties. The morphologies of multi-walled hollow fibers are tailored by controlling the materials and processing parameters such as polymer and solvent types. The triaxial hollow fiber fabrication is achieved through using a nozzle containing concentric tubes, which allows for the transport of different fluids to the tip of the nozzle under the applied high voltage. In comparison to uniaxial electrospun fibers, the hollowness of electrospun fibers enables one to manufacture new reinforcing agents that can improve the specific strength of composites. It is shown that the mechanical properties of epoxy matrix composite incorporated with electrospun fibers as primary fiber reinforcement can be significantly tailored by properly selecting the wall materials, diameters, and the amount of electrospun fibers. We have also presented that triaxial electrospun hollow fibers as co-reinforcement in the glass fiber-laminated epoxy matrix composites enhance the flexural modulus by 6.5%, flexural strength by 14%, the onset of first layer of glass fabric failure strain by 12.5%, and final failure strain by 20%.

Keywords

Core-sheath electrospinning, nanocomposite, triaxial hollow fibers, reinforcing agents

Introduction

Fiber-reinforced advanced composites with thermosetting matrix have emerged as structural materials in applications such as wind turbines, construction, defense, aeronautics, and aerospace due to their high strength, rigidity, and lightweight. The performance of fiber-reinforced composites is mainly controlled by the strength of the fiber–matrix interface and the efficiency of load transfer from the matrix to the reinforcement fiber.[1] However, most of the fiber-reinforced composites do suffer from inadequate interlaminar strength and low fracture toughness, which may cause catastrophic failures without showing any external signs of damage.[2]

Recently, electrospun polymeric fibers with high surface area to volume ratio, tailorable surface functionality, and excellent mechanical performance compared to microfibers of the same material have been considered as an efficient reinforcing material in design and fabrication of polymer matrix composites.[3] Electrospun fibers can be utilized as primary reinforcement as well as co-reinforcement in the presence of

[1]Faculty of Engineering and Natural Sciences, Advanced Composites and Polymer Processing Laboratory (AC2PL), Sabanci University, Istanbul, Turkey
[2]Sabanci University Nanotechnology Research and Application Center, SUNUM, Istanbul, Turkey

Corresponding authors:
Mehmet Yildiz and Yusuf Ziya Menceloglu, Faculty of Engineering and Natural Sciences, Advanced Composites and Polymer Processing Laboratory (AC2PL), Sabanci University, Orhanli–Tuzla, Istanbul 34196, Turkey.
Email: meyildiz@sabanciuniv.edu, yusufm@sabanciuniv.edu

Downloaded from jrp.sagepub.com at Sabanci Universitesi on December 7, 2015

high-performance microfibers such as glass and carbon fabrics.[4,5] Dzenis and Reneker[6] pioneered the utilization of electrospun nanofibrous mat for improving the interlaminar fracture resistance, interlaminar toughness, strength, and delamination resistance of laminated composite materials. Li et al.[7] used polysulfone electrospun mat interlayers to enhance interlaminar fracture toughness of carbon fiber–epoxy composite and reported that the electrospun fibers improve the fracture toughness more efficiently than films prepared by solvent method. In another work, the electrospun polycarbonate nano-interlayers inserted between the plies of laminated composite shifted the onset of delamination to higher stress level by 8.1%, and decreased the numbers of microcracks at the delamination stress by 21.6% and increased the ultimate strength by 9.8%.[8] Zhang et al.[9] demonstrated interlayer toughening of carbon–epoxy composites by using polyetherketone cardo nanofiber membranes electrospun directly onto carbon fabrics. Their results showed that finer nanofiber stabilized the crack propagation during delamination thereby improving the flexure property. They also reported that the increase in the nanofiber interlayer thickness resulted in enhanced Mode I delamination fracture toughness and reduced flexure strength. Bilge et al.[10,11] used chemistry-tuned compatibility of poly(styrene-co-glycidyl methacrylate) nanofibers with epoxy matrix and its ability to confine multi-walled carbon nanotubes (MWCNTs) to increase both flexural strength and flexural modulus up to 25% and 29%, respectively, as well as enhancing the delamination resistance up to 70% in carbon–epoxy-laminated composite.

On the other hand, several research groups have utilized electrospun fibers as primary reinforcing agents in thermosetting matrix. Gao et al.[12] integrated electrospun glass nanofibers into dental composites to increase flexural strength, young modulus, and fracture energy of specimens. Moreover, Lin et al.[13] utilized core–shell nanofibers with the high strength core and the shell with good adhesion to matrix through shell chains interpenetration and entanglement with the cross-linked matrix to create an in situ nano-interface in order to reinforce the bis-glycidyl methacrylate (GMA) dental resin. The strength, Young's modulus, and work of failure were enhanced by 18.7%, 14.1%, and 64.8%, respectively. Ozden et al.[5] studied the reinforcing abilities of three different polymeric electrospun fiber to monitor the effect of glass transition temperature on stiffness of composites. When MWCNT is used as a reinforcing agent in electrospun poly(styrene-co-glycidyl methacrylate), a significant increase in flexural modulus was observed up to 20% compared to neat epoxy.[3]

In the present work, triaxial hollow fibers with two different wall materials and novel architecture are fabricated by using multiaxial electrospinning. Two different polymers, namely, polystyrene (PS) and polymethyl methacrylate (PMMA), both of which are known to have high compatibility with epoxy matrix, are utilized as outer wall of electrospun fibers to improve the strength of the fiber–matrix interface and in turn to increase the efficiency of load transfer from the matrix to the fibers. The middle wall of electrospun fibers is fabricated from polyacrylamide (PAAm) having higher strength than the outer wall material to enhance the mechanical properties of electrospun fibers. Triaxial hollow fibers with different morphology and diameter are produced by tailoring the materials and processing parameters.[14] Classical molding and vacuum infusion techniques are employed to produce hollow fiber-reinforced composites. In classical molding process, the electrospun fiber is used as a primary reinforcement for the epoxy resin. The effect of fiber wall materials, fiber diameter, and fiber content on mechanical performance of epoxy composites is investigated by monitoring flexural properties. In vacuum infusion process, triaxial electrospun fibers are deposited onto glass fibrous mats to form interlayers, and the effect of the interlayers on the mechanical performance of laminated composites is studied extensively.

Experimental

Materials

PMMA and PS (used as epoxy matrix compatible outer wall materials fibers) were synthesized by free radical polymerization of vinyl monomers (30 ml) in the presence of azobisisobutyronitrile (AIBN, 1 g) as the radical initiator in the medium of tetrahydrofuran (THF, 50 ml) at 65°C for 4 h and then, the reaction mixture was precipitated in cold methanol and dried for 12 h in a vacuum oven at 50°C. PAAm as a water-soluble polymer (employed as high-strength inner wall material for fibers) was synthesized by dispersion polymerization of acrylamide monomer (30 g) in methanol (100 ml) by using AIBN (1 g) as an initiator at 65°C. The separation of polymer particles from methanol and monomer mixture was done by vacuum filtration and twice washing the polymer particles with methanol and drying it for 12 h in a vacuum oven at 40°C. Molecular weight (Mw), polydispersity index (PDI), and glass transition temperature (T_g) of these polymers are presented in Table 1. The Mw and PDI of outer wall polymers were determined by Viscotek-VE2001 gel permeation chromatography in N,N-dimethyl formamide (DMF) and the viscosity average molecular Mw of PAAm was measured by Mark–Houwink method. DMF (Sigma–Aldrich, 99%), THF (Merck, 99%), and ethyl acetate (EA, Sigma–Aldrich, 99.5%) were used as

Downloaded from jrp.sagepub.com at Sabanci Universitesi on December 7, 2015

solvents in solution preparation for electrospinning process. Araldite LY 564 resin, Hardener XB 3403, and 0/90 biaxial E-glass-stitched fabrics of Metyx company with the average weight of 313 g/m^2 (161 g/m^2 along the (0°) direction, and 142 g/m^2 along the (90°) direction) were used for the production of laminated composite.

Fabrication of electrospun triaxial hollow fibers

Electrospinning process was performed by using custom made triaxial nozzle and electrospinning setup purchased from *Y*flow Company. The outer and inner diameters of the outer and middle nozzles are, respectively, 2.28/1.7 mm, and 1.4/1.1 mm, while a rod with diameter of 0.7 mm is used as inner part of electrospinning nozzle system to provide hollowness to the electrospun fiber. Prepared solutions for each wall were loaded independently into syringes connected to a nozzle, and the flow rate of each wall material was controlled by separate pumps. The flow rate of outer wall was kept higher than that of middle wall in order to have a complete coverage of middle wall by the outer wall material where flow rates of the outer and inner walls are, respectively, 20 µl/min and 15 µl/min. Electrospinning process was performed using a fixed nozzle to collector distance of 7 cm and tuned applied voltage in the range of 5–30 kV to obtain stable Taylor cone. Figure 1 shows the schematic representation of the triaxial electrospinning setup and process.

Table 1. Mw, PDI, and T_g of outer wall polymers of electrospun fibers.

Polymer	T_g (°C)	Mw (g/mole)	PDI
PMMA	123	326,000	3.2
PS	103	313,000	1.7
PAAm*	189	87,000*	–

Note: Mw, molecular weight; PDI, polydispersity index; T_g, glass transition temperature.
*Viscosity-averaged Mv measured by Mark–Houwink method.

Fabrication and characterization of fiber-reinforced epoxy composites

Two different composite production methods, namely, classical molding and vacuum infusion processes are utilized to prepare hollow fiber-reinforced composites. In the former method, appropriate amount of electrospun fibers are placed into Teflon molds in such a way that the mold surface and height are uniformly covered, and then impregnated by the mixture of degassed resin and hardener system. Subsequently, vacuum oven is employed to remove the entrapped air bubbles from

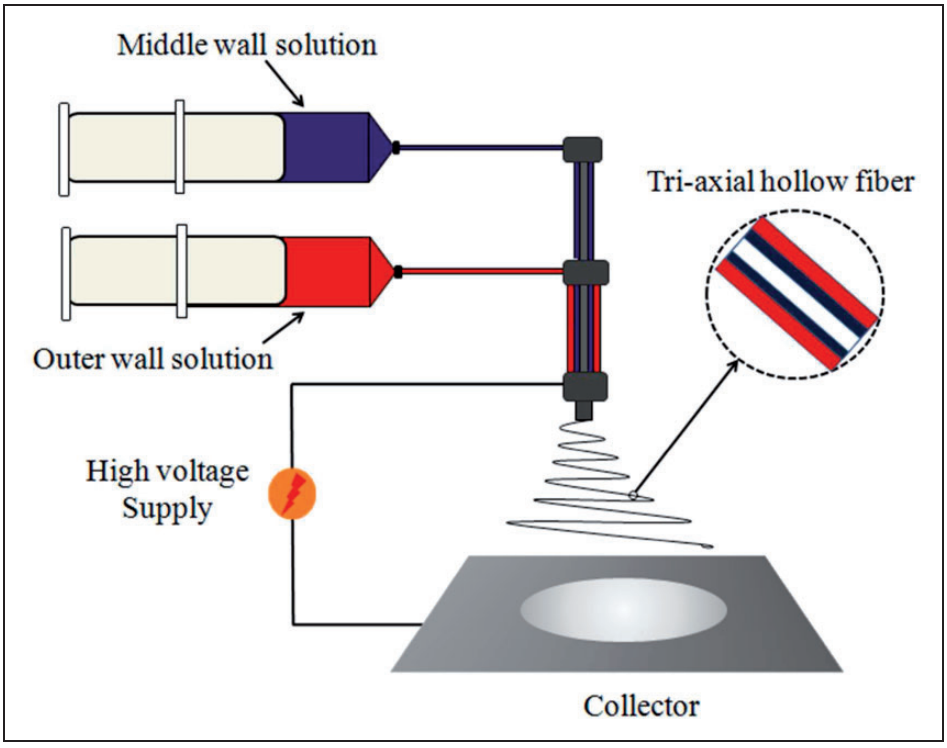

Figure 1. Schematic representation of triaxial electrospinning setup.

Downloaded from jrp.sagepub.com at Sabanci Universitesi on December 7, 2015

the resin and to cure the resin hardener mixture at 50°C for 15 h and post cure at 80°C for 24 h. The electrospun fiber-reinforced molded samples have the length, the width, and the thickness of 100 mm, 14 mm, and 3 mm, respectively, for the three-point bending tests. In order to investigate the effect of electrospun fiber on the mechanical properties of glass fiber-reinforced epoxy matrix composite, triaxial hollow fibers are initially deposited only on the 0° side of the 90°/0° biaxial E-glass stitched fabrics, which are then stacked to form a laminate of $[(90°/0°)_3]_S$. Upon stacking, the electrospun interlayer on the 0° side is shared with the 90° side of the biaxial fabric. The stacked fabrics are impregnated by the epoxy resin after being degassed by vacuum infusion process to manufacture a composite panel with the dimensions of 30 cm × 20 cm × 0.25 cm. The stacking sequence of the plies together with the placement of interlayer, and the schematic of the resin infusion process are given in Figure 2. The weight fraction of the primary reinforcement is 60 wt%, while the weight content of the electrospun fiber is 2 wt%. The volume fractions of glass fiber in the composite laminates were calculated by burning test as nearly 40% of overall composites. The manufactured composite panel is cut to flexural and tensile test specimens with the dimensions of 8 cm × 1.5 cm × 0.25 cm, and 16 cm × 2 cm × 0.25 cm (with the gage length of 10 cm), respectively, which are then tested to evaluate their mechanical properties. To avoid the breakage of tensile specimens at grip locations, both ends of specimens are tabbed with an aluminum tab having a dimension of 3 cm × 2 cm × 0.1 cm using two-component room temperature curing epoxy system (Araldite, 2011). Flexural and tensile tests are repeated three times for each type of specimens.

A detailed fractographic analysis was carried out in order to identify the failure mechanisms of composites on the cross section along the length of the specimen through thickness. Both flexural and tensile test specimens are cut such that the length of the specimens is aligned with the direction of weft fibers as shown in Figure 2(a) where the yellow-painted region illustrates the cut specimen for flexural and tensile tests. A specific custom-made apparatus is used to stabilize the displacement of composites after three-point bending test[15] and then these specimens are directly immersed into the fast-curing resin–hardener mixture and thus the specimens preserve the displacement after curing. Figure 3 represents step-by-step procedure followed for the preparation of samples for fractographic analysis. Figure 3(a) exhibits the cut specimen of the glass fiber-reinforced composite modified by multi-walled hollow polymeric fibers and apparatus that is used in this characterization technique. In Figure 3(b), specimen is fixed with desired displacement into the apparatus and in Figure 3(c) and (d), the specimen fixed by the apparatus is immersed into the fast curing hardener and epoxy mixture to preserve the displacement after curing. Figure 3(e–h) illustrate the specimen after the surrounding epoxy hardener mixture has been cured, and after the specimen is cut into the desired geometry

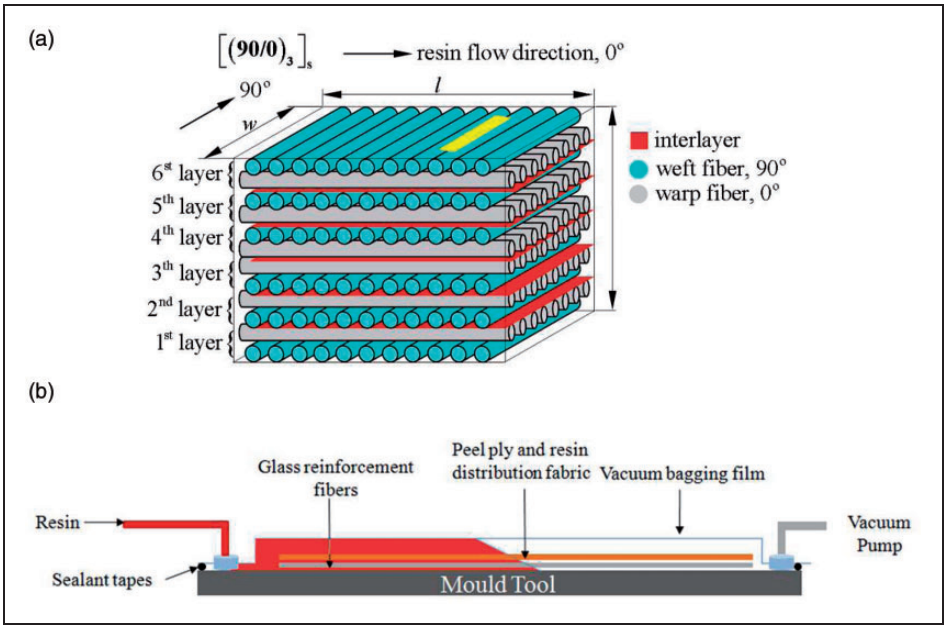

Figure 2. A schematic representation of composite manufacturing by vacuum infusion, (a) stacking sequence and the placement of the interlayer where the yellow region indicates the cut specimen for flexural and tensile tests, and (b) the vacuum infusion system.

Downloaded from jrp.sagepub.com at Sabanci Universitesi on December 7, 2015

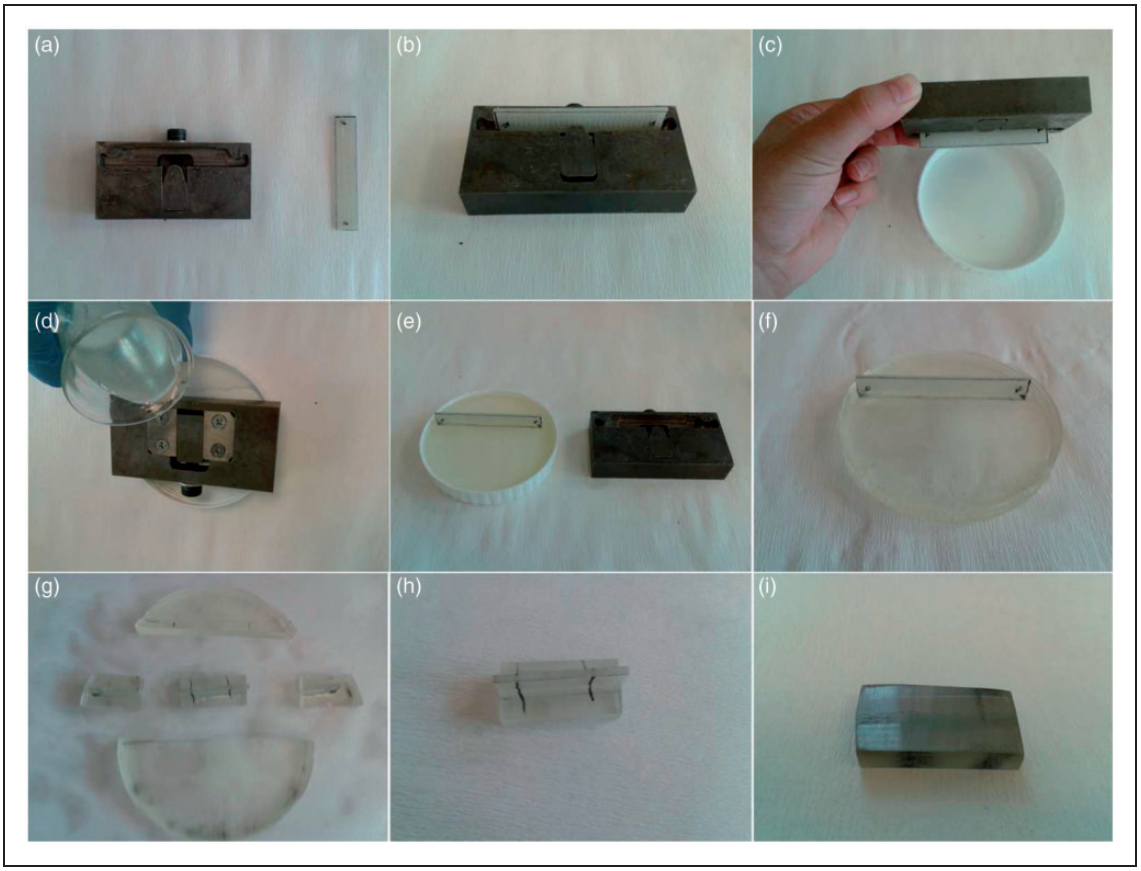

Figure 3. Step-by-step procedure followed for sample preparations for the analysis of failure mechanisms.

for the next step. The cut specimen containing failure area of three-point bending specimen is polished and then coated with Au/Pd for scanning electron microscope (SEM) characterization (Figure 3(i)).

The surface morphologies of fibers and cross-sectional area of specimens after breakage were analyzed by a Leo Supra 35VP field emission SEM. The mechanical tests were conducted by using ZWICK Proline 100 Universal Test Machine with 10 and 100 kN load cells for three-point bending and tensile tests, respectively, using a constant cross-head speed of 2 mm/min. ASTM D790-03 and ASTM D5083—02 standards are used for three-point bending and tensile tests to measure mechanical properties of composite samples, respectively. Dynamic Mechanical Analyzer (DMA) (Netzsch DMA 242 C) is used to analyze mechanical properties of the composite as a function of temperature, time, and frequency.

Results and discussion

Surface morphologies of triaxial hollow fibers

Three different types of triaxial hollow electrospun fiber were fabricated to investigate the effect of the type of outer layer polymer, and fibers diameter on the mechanical properties of composites, namely, PMMA/PAAm hollow fibers fabricated by using two different outer wall solvents (i.e., DMF and EA) and PS/PAAm hollow fibers with the outer wall solvent of EA. Figure 4 exhibits the fiber morphology of triaxial hollow electrospun fibers with outer wall of PMMA and PS and inner wall of PAAm. The effect of solvent type on fiber morphology during electrospinning process is also investigated. When DMF is used as an outer wall solvent in PMMA, the resulting fiber diameter is about 100 nm as shown in Figure 4(a). On the other hand, higher vapor pressure of EA as outer wall solvent in PMMA leads to the formation of fibers with diameter larger than 500 nm as can be seen in Figure 4(b). As discussed in detail in our previous paper,[16] the polymeric jet of the outer wall solution prepared by using low vapor pressure solvent is subjected to the instabilities of electrospinning process at longer time and thus, the diameter of fibers is reduced before reaching the surface of the collector. On the other hand, the utilization of higher vapor pressure solvent results in faster drying of polymeric jet during electrospinning, thereby producing fibers with a larger diameter.

Downloaded from jrp.sagepub.com at Sabanci Universitesi on December 7, 2015

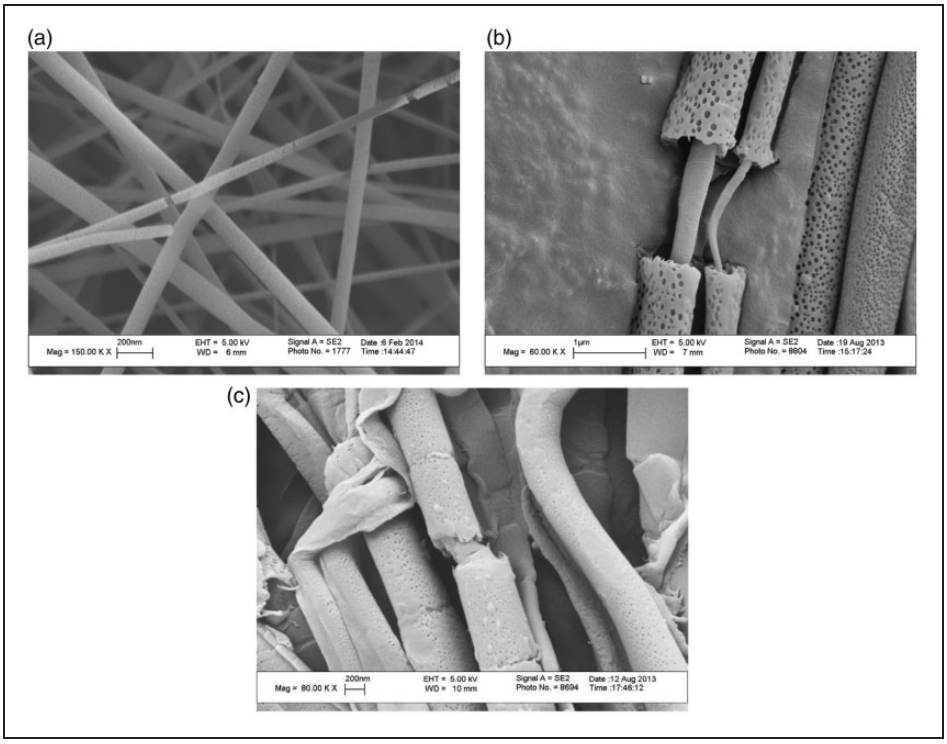

Figure 4. SEM images of triaxial hollow electrospun fibers of (a) PMMA/PAAm fibers fabricated by outer wall solvent of DMF, (b) PMMA/PAAm fibers fabricated by outer wall solvent of EA and (c) PS/PAAm fibers fabricated by outer wall solvent of EA.

During the handling of the electrospun fiber mat, it was observed that increasing the solvent pressure makes fibers more brittle. This observation can be substantiated as follows. Note that multi-walled fibers with smaller and larger diameters produced by the same wall materials are expected to have the similar strain values at breakage. Defining the strain as $\varepsilon = d/r$ where d is the fiber diameter and r is the radius of curvature due to the bending, one can readily infer that the fiber having a larger diameter should break with the bigger radius of curvature, hence giving rise to more brittle behavior, whereas fibers with smaller diameter should be capable of being bent to smaller radius of curvature, thus evoking more bending capabilities. Figure 4(c) represents triaxial hollow electrospun fiber with outer wall of PS and the diameter of these fibers is almost same as the one having the outer wall polymer of PMMA synthesized by EA solvent shown in Figure 4(b).

Flexural properties of triaxial hollow fiber-reinforced composites

The effect of outer wall material of triaxial hollow fiber. The interfacial interactions between outer wall of electrospun fiber and polymer matrix play a critical role to transfer the load from matrix to the reinforcing agent thus improving the mechanical properties of composite. Herein, different outer wall materials are used to tailor the interface properties of electrospun fibers and to provide the best possible interface between electrospun fibers and epoxy matrix. Figure 5 presents a comparison of stress–strain curves of electrospun fiber-reinforced composite specimens and neat epoxy specimens. The flexural modulus of PS–PAAm triaxial hollow fiber-reinforced composite slightly increases, while the brittleness of the specimens increases significantly which can be noted upon comparing the strains at fracture for PS–PAAm reinforced and neat specimens that are nearly $7 \pm 0.5\%$ and $14 \pm 0.3\%$, respectively. Moreover, referring to flexural strengths of PS–PAAm, triaxial hollow fiber-reinforced and neat specimens, which are respectively 79 ± 0.5 MPa and 75 ± 0.4 MPa, one can see that PS–PAAm triaxial hollow fibers increase the load-bearing capacity of the matrix. The PMMA–PAAm triaxial hollow fiber-reinforced composite also shows an increase in flexural modulus and yield strength in comparison to specimens reinforced by PS–PAAm triaxial hollow fibers. This can be attributed to better interfacial compatibility between the PMMA wall of electrospun fibers and epoxy matrix, which can be further elaborated as follows. As depicted in Figure 6, PMMA chains in outer shell of electrospun fibers are partially dissolved thereby interpenetrating into epoxy and hardener mixture, resulting in the entanglement of linear PMMA chains with the cross-linked matrix network and hence the

Downloaded from jrp.sagepub.com at Sabanci Universitesi on December 7, 2015

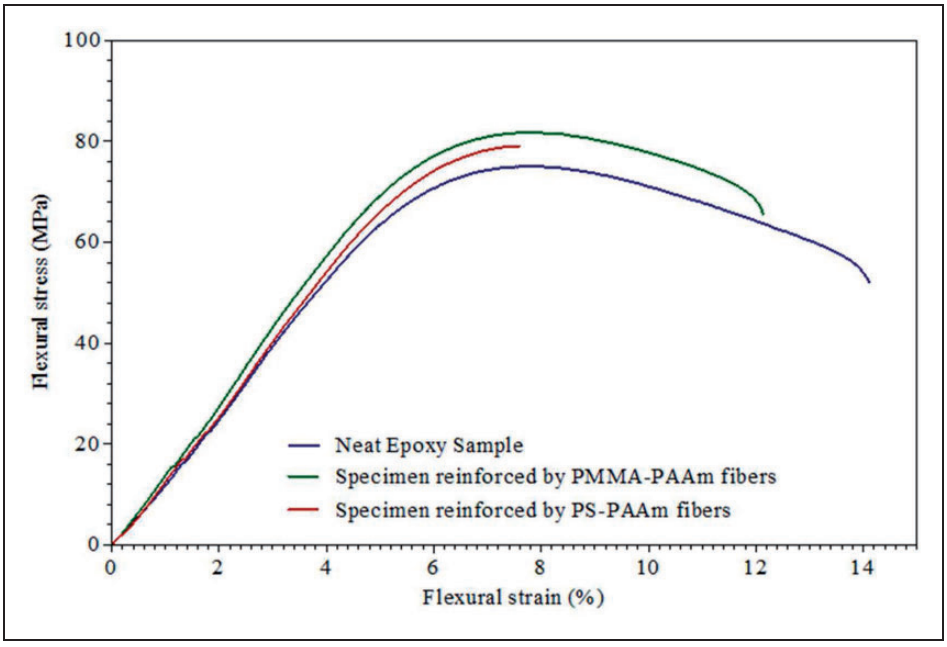

Figure 5. Flexural stress–strain curves of samples for neat epoxy and samples reinforced by 0.2 wt% PSPAAm and 0.2 wt% PMMA–PAAm triaxial hollow fibers. Both fibers are produced with the outer layer solvent of EA and inner layer solvent of water.

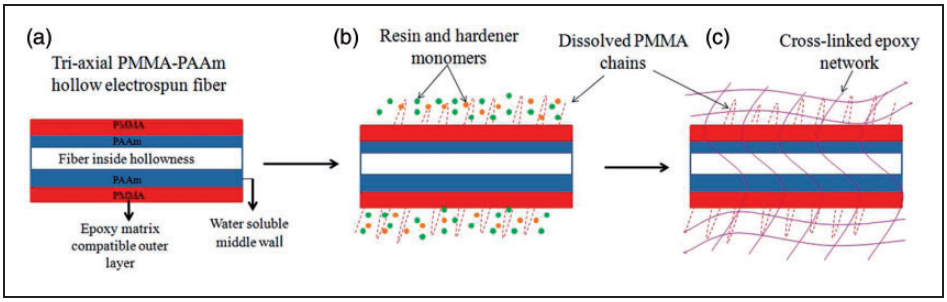

Figure 6. Schematic representation of semi-IPN structure formation in PMMA–PAAm triaxial hollow fiber-reinforced composite: (a) PMMA–PAAm triaxial hollow fiber, (b) partial dissolution of PMMA shell into the resin and hardener mixture, and (c) semi-IPN structure formation.

formation of semi-interpenetrating polymer network (semi-IPN) structure, which lends itself to an improved load transfer between matrix and electrospun fibers.[13]

The effect of fiber diameter. The diameter of electrospun reinforcing fibers is another critical parameter affecting the mechanical properties of the composite. In Figure 7 illustrates the stress–strain curves for composites reinforced by PMMA–PAAm triaxial hollow fibers of different diameters while keeping the electrospun fiber content constant for both cases at 0.2 wt%. PMMA–PAAm triaxial hollow fibers with an average diameter of 100 nm increase the modulus of composite specimen up to 1.72 ± 0.03 Gpa, which is significantly higher than the modulus of 1.44 ± 0.02 GPa obtained for specimen reinforced by fibers with an average diameter of 500 nm. Moreover, electrospun fibers with an average diameter of 100 nm increase flexural strength of specimens up to 91 ± 0.4 MPa. This improvement in the flexural properties of composites is attributed to the increase in specific surface area of electrospun fibers due to the decrease in the diameter, which enhances the interactions between the electrospun fibers and the matrix, thereby leading to better load transfer between them. On the other hand, finer electrospun fibers shift the failure strain to lower strain levels, which might be attributed to the increase in the number of interface in the composites that can act as crack initiation or stress concentration sites.

The effect of fiber content. The effect of electrospun fiber amount on the flexural properties of specimens is also

Downloaded from jrp.sagepub.com at Sabanci Universitesi on December 7, 2015

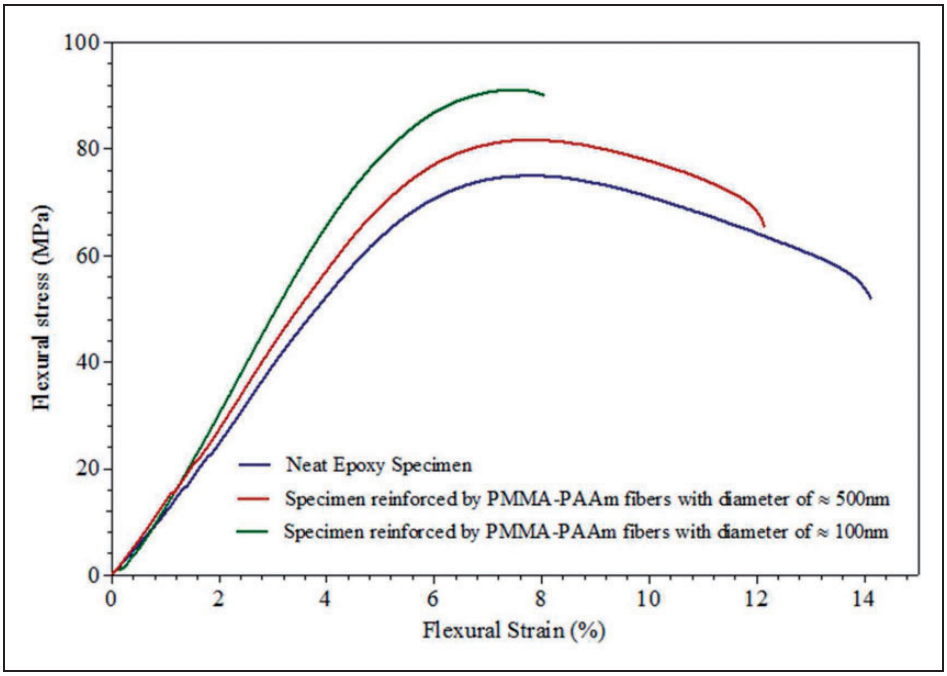

Figure 7. Flexural stress–strain curves of neat epoxy sample and samples reinforced by PMMA–PAAm triaxial hollow fibers with different fiber diameters.

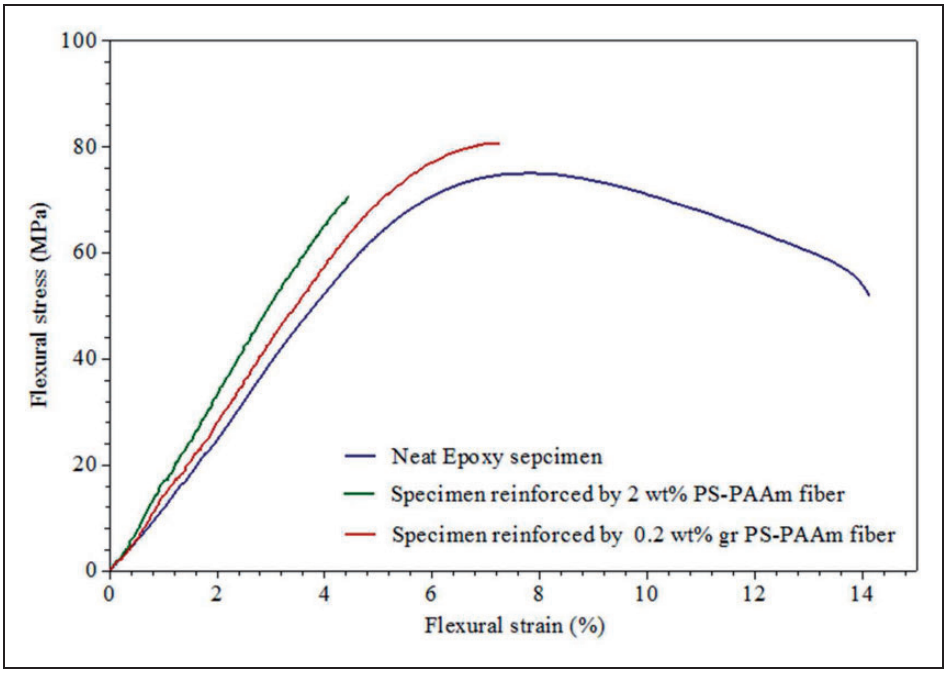

Figure 8. Flexural stress–strain curves of neat epoxy specimen and specimens reinforced with 0.2 wt% and 2 wt% PS–PAAm triaxial hollow fiber.

investigated by comparing two different fiber contents of 2 and 0.2 wt%. Figure 8 reveals an increase in flexural modulus of specimens even with low fiber content of 0.2 wt%, whereas raising the fiber content to 2 wt% further increases the modulus up to 1.63 ± 0.02 GPa from the value of 1.34 ± 0.01 for neat epoxy specimens. The notable rise in the modulus upon increasing the fiber content is explained by augmenting the accessible interfaces between reinforcing electrospun fibers inside the specimens with epoxy matrix, thereby leading to

Downloaded from jrp.sagepub.com at Sabanci Universitesi on December 7, 2015

Table 2. Improvements in the flexural strength and modulus of hollow fibers reinforced composites in percentage.

Reinforcement	PMMA–PAAm hollow fiber	PS–PAAm hollow fiber	PMMA–PAAm hollow fiber	PS–PAAm hollow fiber
Fiber diameter (nm)	500	500	100	500
Reinforcement amount (wt%)	0.2	0.2	0.2	2
Flexural strength (MPa)	82 ± 0.3	79 ± 0.5	91 ± 0.4	70.5 ± 0.5
Flexural strength improvement (%)	9.3 ± 1	5.3 ± 1.2	21.3 ± 1.2	-5.9 ± 1.2
Flexural modulus (GPa)	1.44 ± 0.02	1.38 ± 0.02	1.72 ± 0.03	1.63 ± 0.02
Flexural modulus improvement (%)	7.4 ± 2.2	2.3 ± 0.7	28.4 ± 3.2	21.6 ± 0.5

Note: PMMA, polymethyl methacrylate; PAAm, polyacrylamide; PS, polystyrene.

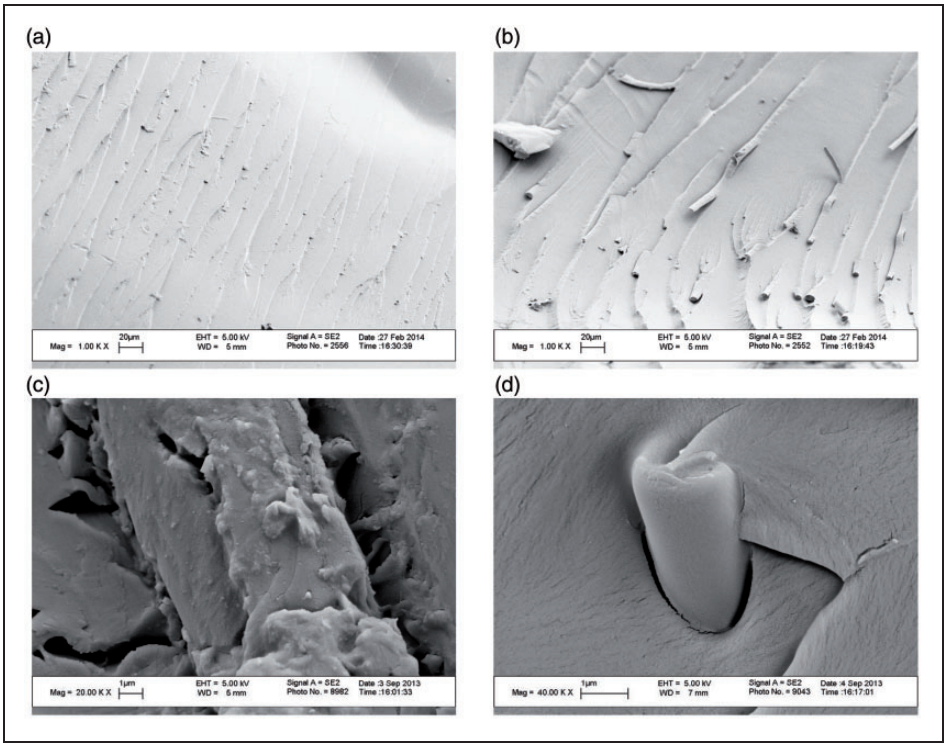

Figure 9. SEM images of fracture surface of specimens after three-point bending tests, (a) neat epoxy, (b) PMMA/PAAm triaxial hollow fiber-reinforced composite with the outer layer solvent of EA and (c,d) close-up view for PMMA–PAAm triaxial hollow fiber-reinforced composite.

further load transfer to fibers and increasing the modulus. It is also observed that increasing the fiber amount changes the behavior of specimens from ductile to brittle behavior and specimens start to get damaged at lower strain levels, which again can be attributed to the increase in the number of interfaces possibly acting as crack initiation or stress concentration points.

Table 2 summarizes flexural strength and flexural modulus of hollow fibers reinforced composites in terms of percentages. The results show that hollow fibers with outer wall of PMMA and the fiber diameter of 100 nm significantly enhance flexural strength and flexural modulus of composite.

Fracture surface analysis of hollow fiber-reinforced composites

Figure 9 gives SEM images for the fracture surfaces of neat epoxy samples and electrospun fiber-reinforced composites subjected to three-point bending tests. In general, the fracture surface of the electrospun fiber-reinforced sample looks rougher and more fragmented than that of the neat one. Figure 9(c) exhibits the

Downloaded from jrp.sagepub.com at Sabanci Universitesi on December 7, 2015

formation of semi-IPN structure around electrospun fibers, which increase the fiber diameter as well as covers the fiber with thick layer of cross-linked epoxy resin, thus providing higher interfacial interaction and load transfer between the electrospun fibers and epoxy matrix. Figure 9(d) shows the breakage of electrospun fibers at failure area of specimen.

Laminated glass fiber-reinforced composites by hollow fibers

In Figure 10, the flexural properties obtained from three-point bending test shows minor enhancement in flexural modulus from 10.8 ± 0.2 GPa for conventional glass-fiber reinforced specimens up to 11.5 ± 0.2 GPa for samples modified by PMMA–PAAm triaxial hollow fibers interlayers electrospun with the outer wall solvent of DMF. As can be seen from Figure 10, there are some sudden changes in stress values at higher stress and strain ranges associated with failure of individual reinforcing glass fiber plies. The first sudden drop in the stress value is considered as the breakage of first layer of glass fibers. The presence of PMMA–PAAm triaxial hollow fibers interlayers improves the breakage strain of first layer of glass fibers by around 12.5%. Furthermore, the complete failure of electrospun modified samples is shifted to higher strain level by nearly 20%. The flexural strength of electrospun fiber-integrated specimen increases by 14%. Referring to results in Figure 11, one may note that there is no change in tensile properties between neat and electrospun interlayers integrated glass fiber-reinforced epoxy composite specimens. The significant difference between the results of flexural and tensile tests might be attributed to the dissimilarity in the breakage mechanisms for the flexural and the tensile tests. During the flexural test, primary glass fibers are bent perpendicular to the direction of the applied force and in turn damaged leading to formation of cracks, which propagate across the plies of the primary reinforcement. The interlayers between the plies of the primary reinforcement stabilize the crack propagation through arresting cracks, thereby giving rise to toughening. However, during tensile test, the direction of applied force is through the plane of matrix and cracks are formed transversely in the plane of plies and not across the plies, hence electrospun interlayers cannot act as efficient crack stabilizer. As well, the tensile strength of the electrospun fibers is significantly inferior to glass fibers. Thus, the contribution of the electrospun interlayer to axial load-bearing capacity is negligible in comparison to primary glass fiber reinforcement. The current result of the tensile tests can alternatively be interpreted such that the interlayer does not imperil the tensile properties of composite structure through acting as defects at the interface regions of the composite laminas.

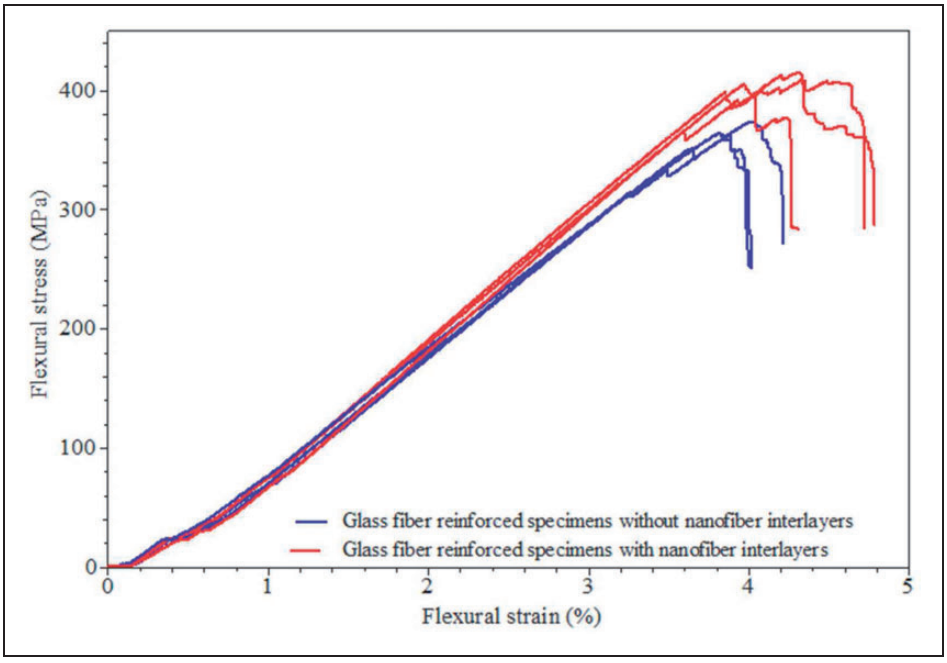

Figure 10. Flexural stress–strain curves of glass fiber-reinforced epoxy specimen and specimen modified by interlayers of triaxial hollow fibers of PMMA–PAAm.

Downloaded from jrp.sagepub.com at Sabanci Universitesi on December 7, 2015

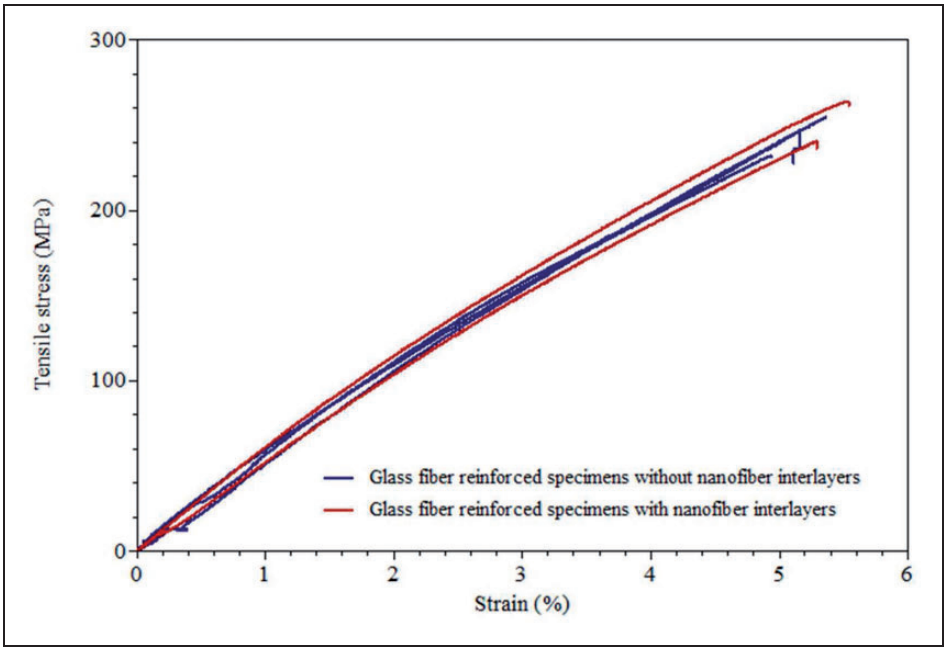

Figure 11. Tensile stress versus strain curves of glass fiber-reinforced epoxy specimen and specimen modified by interlayers of triaxial hollow fiber of PMMA–PAAm.

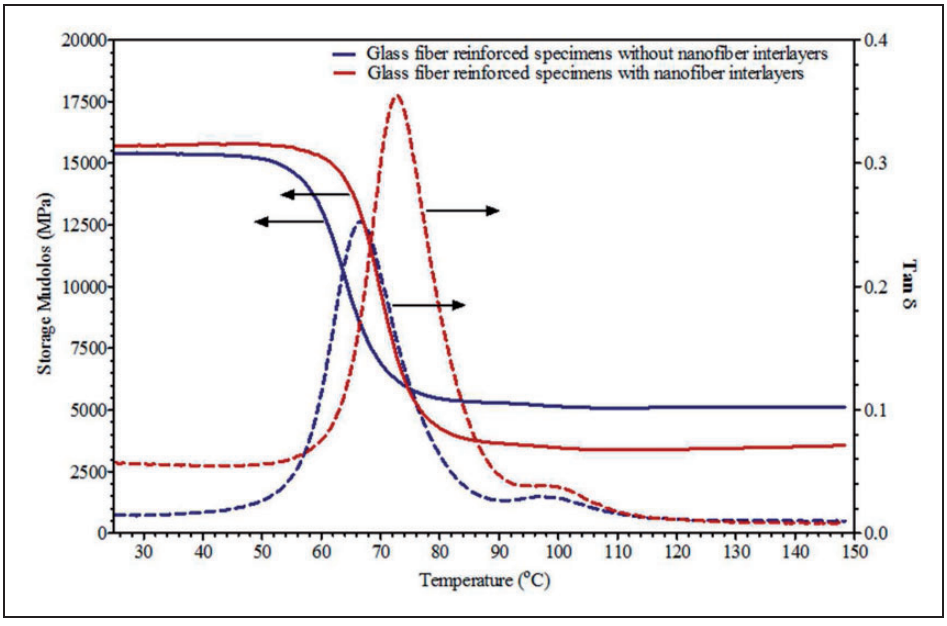

Figure 12. Tan δ and E′ curves of glass fiber-reinforced specimens with and without nanofiber interlayers.

Dynamic mechanical properties of glass fiber-reinforced composites

DMA analyzes the viscoelasticity of a material by applying a sinusoidal force or displacement and measuring the corresponding response. The storage modulus, E', is proportional to the energy stored per cycle (elastic behavior), while the loss modulus, E'', is associated with the dissipated energy per cycle (viscous behavior).[17] Tan delta (δ) is a damping term that is defined as the ratio of the loss modulus to the storage modulus, and the temperature corresponding to the tan δ peak is often related to the glass transition temperature (T_g). Figure 12 shows DMA results of specimens

Downloaded from jrp.sagepub.com at Sabanci Universitesi on December 7, 2015

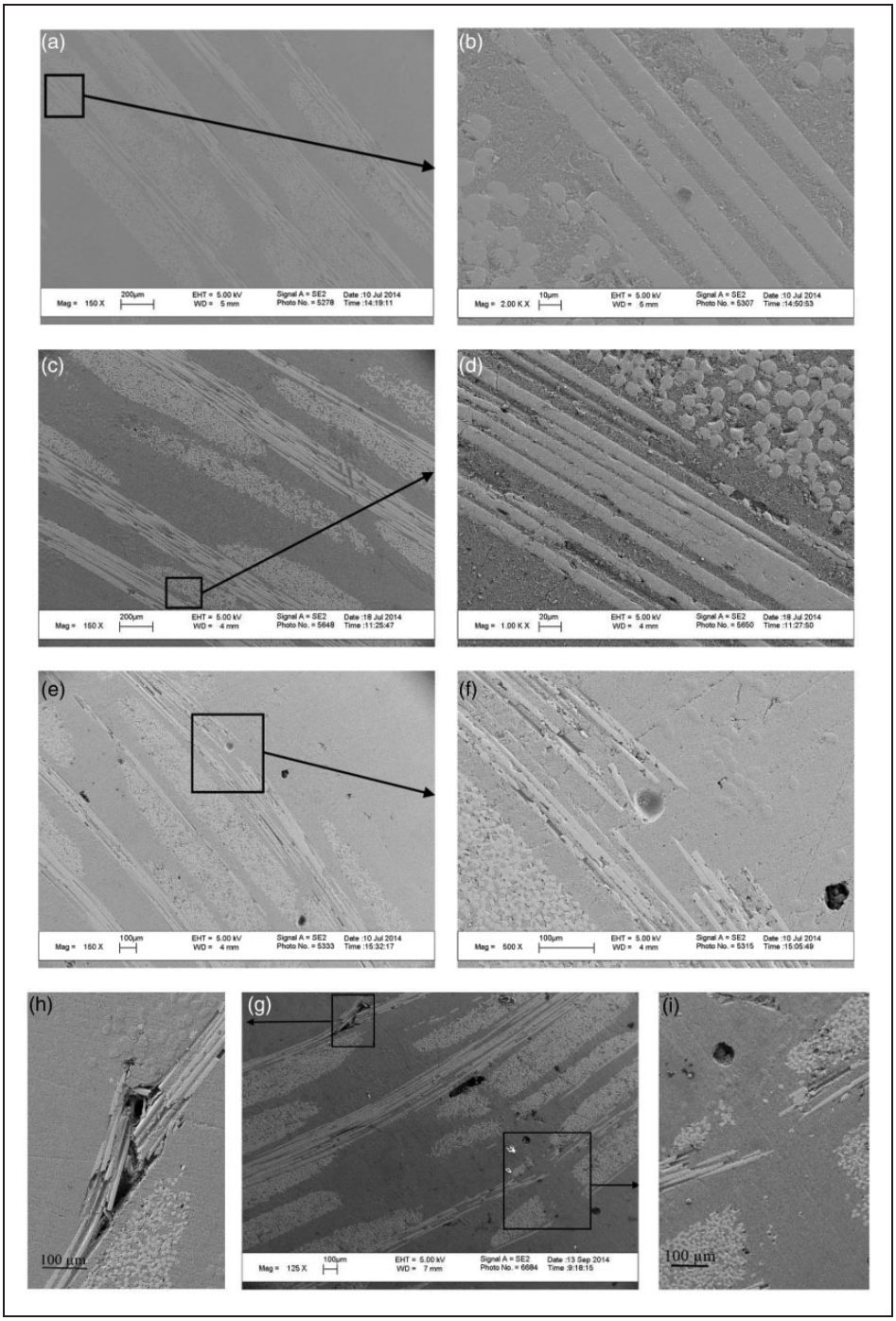

Figure 13. SEM images of cross-sectional area of (a,b) glass fiber-reinforced epoxy specimen without nanofiber interlayers before applying load, (c,d) glass fiber-reinforced epoxy specimen modified by nanofiber interlayers before applying load, (e,f) glass fiber-reinforced specimen without nanofiber interlayers after bending, (g–i) glass fiber-reinforced specimen modified by nanofiber interlayers after bending.

with and without nanofiber interlayers. Referring to the tan δ curves of composites in this figure, T_g of composite specimen with nanofibers ($T_g = 73°C$) is greater than that of neat composite ($T_g = 66°C$). This increase stems from semi-IPN formed through the entanglement of linear PMMA chains having a T_g of 123°C with crosslinked epoxy matrix with lower T_g[18] since semi-IPN structure may restrict the segmental motion of the matrix leading to higher energy requirement for the glass transition.[19] The increase in T_g of the composite makes it also suitable for high temperature engineering applications. The significant increase in tan δ peak of nanofiber-modified

Downloaded from jrp.sagepub.com at Sabanci Universitesi on December 7, 2015

specimen might be attributed to the presence of thermoplastic nanofiber interlayers, which experience increasing chain mobility at higher temperature. In addition, the storage modulus of specimen with nanofiber interlayers at glassy region (before T_g) is higher than the neat specimen since electrospun fibers provide strong interfacial adhesion between glass fibers and epoxy matrix, which is also in agreement with the result of flexural tests at room temperature. The storage modulus of specimen laminated with nanofibers in rubbery region (after T_g) is lower than that of neat specimen due to the presence of thermoplastic polymeric hollow fibers at the interface of matrix and glass fibers and higher viscous behavior of these hollow fibers than thermoset matrix at elevated temperature.

Microscopic observation and failure mechanisms

To investigate the failure mechanisms of composites, a fractographic analysis is performed on the cross section of flexural test specimens (bounded by length and the thickness). Figure 13 represents SEM images of cross-sectional areas of flexural test specimens after cutting and polishing steps. The cross section corresponds to the right-hand side view of Figure 2(a). Therefore, in the SEM images, the most outer fibers are parallel to the image plane. In these specimens, there are three distinct regions; namely, fibers oriented in a parallel manner to the cross section plane, fibers oriented perpendicularly to cross section plane, and matrix-rich regions. Figure 13(a) demonstrates the cross section of neat glass fiber-reinforced specimen before applying any force or displacement and Figure 13(b) presents a close-up view for the boxed region in Figure 13(a). Figure 13(c) and (d) exhibit the cross section of specimens laminated with triaxial hollow fibers before bending. SEM images of both specimens before the application of flexural force confirm that fibers are satisfactorily wetted by matrix. The failure behaviors of both neat specimen and specimen with triaxial hollow fibers after bending are shown in Figure 13(e–i). In Figure 13(e) and (f), only the first outer layer (specimen surface at the support side) of the neat specimen is broken down after bending. On the other hand, higher stress is required to break down the layers of specimen laminated with triaxial hollow fibers and after bending, cracks start at both inner (Figure 13(h)) and outer layers, and the crack initiated at outer layer (Figure 13(i)) propagates toward inner layers (Figure 13(g)).

Conclusions

Novel architecture of triaxial electrospun hollow fibers with controlled diameter and morphology is fabricated by multiaxial electrospinning technique. The effect of electrospun fibers with different wall materials, morphology, diameter, and fiber content on the mechanical performance of composite specimens is studied. Two different composite production techniques which are casting onto a Teflon mold and vacuum infusion are applied to produce composite structures. Some of the most important findings of the current study might be concisely summarized as;

- Electrospun fibers with PMMA outer shell enhance the flexural modulus and strength without affecting the toughness of samples, whereas PS outer wall enhances the flexural modulus and strength at the expense of reducing the toughness.
- Specimens reinforced by finer electrospun fibers show higher enhancement in flexural modulus at the price of shifting the failure strain to lower strain levels.
- The increase in the amount of electrospun fibers augments accessible interfaces between reinforcing electrospun fibers and epoxy matrix in composites, thereby improving load transfer capability and in turn the flexural modulus of the composites. However, the associated increase in the stress concentration points due to the higher number of interfaces degrade the flexural strength as well as strain at breakage.
- The utilization of PMMA–PAAm hollow fiber as inter layers of glass fiber-laminated composites, enhances the flexural modulus by 6.5%, flexural strength by 14%, the onset of first layer of glass fabric failure strain by 12.5%, and final failure strain by 20%. DMA results for glass fiber-reinforced specimens laminated with nanofiber interlayers show 7°C increase in T_g in comparison to neat specimens. Especially, these improvements in conventional glass fiber composites open up new way to produce more reliable and long-lasting composites. Consequently, hollow fiber reinforcement is a promising material for the production of advance composites with ultra lightweight, multifunctionality and an improved structural performance.

The future studies will involve the integration of nanoparticles into the outer layer of multi-walled hollow fibers to further enhance the performance of epoxy composites. Also, the desired materials can be encapsulated inside the hollow fibers in a single step during electrospinning process, which will bring additional functionalities into epoxy composite structures such as vascular self-healing.

Acknowledgements

The authors thank to Cagatay Yilmaz, Ataman Deniz, and Esat Selim Kocaman for their help in the preparation of composite samples.

Downloaded from jrp.sagepub.com at Sabanci Universitesi on December 7, 2015

Conflict of interests

None declared.

Funding

The authors gratefully acknowledge financial support from the Scientific and Technical Research Council of Turkey (TUBITAK) with the project numbers of 112M312/COST MP1202 and 112M357.

References

1. Godara A, Gorbatikh L, Kalinka G, et al. Interfacial shear strength of a glass fiber/epoxy bonding in composites modified with carbon nanotubes. *Compos Sci Technol* 2010; 70: 1346–1352.
2. Lubineau G and Rahaman A. A review of strategies for improving the degradation properties of laminated continuous-fiber/epoxy composites with carbon-based nanoreinforcements. *Carbon* 2012; 50: 2377–2395.
3. Ozden-Yenigun E, Menceloglu YZ and Papila M. MWCNTs/P(St-co-GMA) composite nanofibers of engineered interface chemistry for epoxy matrix nanocomposites. *ACS Appl Mater Interf* 2012; 4: 777–784.
4. De Schoenmaker B, Van der Heijden S, De Baere I, et al. Effect of electrospun polyamide 6 nanofibres on the mechanical properties of a glass fibre/epoxy composite. *Polym Testing* 2013; 32: 1495–1501.
5. Ozden E, Menceloglu YZ and Papila M. Engineering chemistry of electrospun nanofibers and interfaces in nanocomposites for superior mechanical properties. *ACS Appl Mater Interf* 2010; 2: 1788–1793.
6. Dzenis YA and Reneker DH. Delamination resistant composites prepared by small diameter fiber reinforcement at ply interfaces. Google Patents, 2001.
7. Li G, Li P, Zhang C, et al. Inhomogeneous toughening of carbon fiber/epoxy composite using electrospun polysulfone nanofibrous membranes by in situ phase separation. *Compos Sci Technol* 2008; 68: 987–994.
8. Sihn S, Kim RY, Huh W, et al. Improvement of damage resistance in laminated composites with electrospun nanointerlayers. *Compos Sci Technol* 2008; 68: 673–683.
9. Zhang J, Lin T and Wang XG. Electrospun nanofibre toughened carbon/epoxy composites: effects of polyetherketone cardo (PEK-C) nanofibre diameter and interlayer thickness. *Compos Sci Technol* 2010; 70: 1660–1666.
10. Bilge K, Ozden-Yenigun E, Simsek E, et al. Structural composites hybridized with epoxy compatible polymer/MWCNT nanofibrous interlayers. *Compos Sci Technol* 2012; 72: 1639–1645.
11. Bilge K, Venkataraman S, Menceloglu YZ, et al. Global and local nanofibrous interlayer toughened composites for higher in-plane strength. *Compos Part A-Appl S* 2014; 58: 73–76.
12. Gao Y, Sagi S, Zhang L, et al. Electrospun nano-scaled glass fiber reinforcement of bis-GMA/TEGDMA dental composites. *J Appl Polym Sci* 2008; 110: 2063–2070.
13. Lin S, Cai Q, Ji J, et al. Electrospun nanofiber reinforced and toughened composites through in situ nano-interface formation. *Compos Sci Technol* 2008; 68: 3322–3329.
14. Monfared Zanjani JS, Okan BS, Yildiz M, et al. Fabrication and morphological investigation of multi-walled electrospun polymeric nanofibers. *MRS Proc* 2014; 1621: 119–126.
15. Demircan Ö, Ashibe S, Kosui T, et al. Mechanical properties of biaxial weft-knitted and cross-ply thermoplastic composites. *J Thermoplast Compos Mater* 2014: 0892705713519119.
16. Seyyed Monfared Zanjani J, Saner Okan B, Letofsky-Papst I, et al. Rational design and direct fabrication of multi-walled hollow electrospun fibers with controllable structure and surface properties. *Eur Polym J* 2015; 62: 66–76.
17. Goertzen WK and Kessler MR. Dynamic mechanical analysis of carbon/epoxy composites for structural pipeline repair. *Compos Part B: Eng* 2007; 38: 1–9.
18. Kalogeras IM and Brostow W. Glass transition temperatures in binary polymer blends. *J Polym Sci Part B: Polym Phys* 2009; 47: 80–95.
19. Hossain KMZ, Ahmed I, Parsons AJ, et al. Physico-chemical and mechanical properties of nanocomposites prepared using cellulose nanowhiskers and poly(lactic acid). *J Mater Sci* 2012; 47: 2675–2686.

Downloaded from jrp.sagepub.com at Sabanci Universitesi on December 7, 2015